Intrinsic Reaction Coordinate Analysis of the Activation of CH_4 by Molybdenum Atoms: A Density Functional Theory Study of the Crossing Seams of the Potential Energy Surfaces

Zhen Guo,[†] Zhuofeng Ke,[‡] David Lee Phillips,*[,†] and Cunyuan Zhao*[,‡]

Department of Chemistry, The University of Hong Kong, Pokfulam Road, Hong Kong, P. R. China, and School of Chemistry and Chemical Engineering, Sun Yat-Sen University, Guangzhou 510275, P.R. China

Received July 23, 2007

Density functional theory (DFT) calculations were performed to investigate the quintet, triplet, and singlet potential energy surfaces associated with the C-H activation of methane by laser-ablated molybdenum (Mo) atoms recently observed experimentally by Andrews and co-workers. The present computational study aims to better understand the nature of the reaction mechanisms for C-H activation by Mo atoms. The processes for activation of methane by the excited Mo atoms appear to produce CH_3—MoH, CH_2═MoH_2, and CH≡MoH_3 complexes. The crossing seams between the potential energy surfaces and possible spin inversion processes for the direct conversion of methane to a high oxidation state transition metal complex that contains a carbon-metal double or triple bond are examined using the intrinsic reaction coordinate (IRC) approach. The minimum energy reaction pathway is found to involve spin inversion three times in different reaction steps. In total, three spin states (quintet, triplet, and singlet) are involved in going from the entrance channel to the exit channel: $^5Mo + CH_4 \rightarrow CH_3$—MoH (^{5}**1**) → CH_2═MoH_2 (^{3}**2**) → CH≡MoH_3 (^{1}**3**). The first crossing seam exists prior to $\mathbf{TS_{1-2}}$, a three-centered transition state for the H-transfer of complex **1** to form a double carbon-metal bond complex **2**. This crossing seam is a key aspect in the reaction pathway because the molecular system should change its spin multiplicity from the quintet state to the triplet state near this crossing region, which leads to a significant decrease in the barrier height of $\mathbf{TS_{1-2}}$ from 51.0 to 33.8 kcal mol^{-1} at the B3LYP level of theory. The second crossing seam between the quintet potential energy surface (PES) and the singlet PES is found not to play a significant role because the triplet potential energy surface lies significantly below the quintet and singlet potential energy surfaces. Accordingly, the molecular system would preferentially move on the triplet potential energy surfaces before encountering the second seam. The crossing seam between the triplet exit channel and the singlet exit channel can take place, in which complex ^{1}**3** containing a triple carbon-metal bond is formed via an H-transfer process. This crossing seam will again lead to a spin inversion from the triplet to the singlet state, and this leads to a large decrease in the height of the reaction barrier from 40.8 to 17.2 kcal mol^{-1}.

1. Introduction

The selective transformation of common inert C-H bonds of alkanes such as methane to other functional groups by neutral transition metals and their ions to give high oxidation state transition metal complexes has been motivated by both interest in the fundamental aspects of the chemistry and the potential economic and environmental impact of this chemistry.[1] Thus, there has been a great deal of experimental and theoretical work done in this area, which has resulted in many examples in the literature of C-H bond activation at transition metal centers.[1–5] In order to develop practical alkane conversion processes, the process and factors controlling the activity and selectivity of catalytic alkane activation needs to be better understood. Methane is a useful starting point because it is the simplest hydride of carbon and the principal constituent of natural gas. Thus, the activation of methane by a transition metal cation, M^+, or a neutral transition metal, M, has been the subject of a number of studies.[6–11] It is very important to understand the nature of metal coordination of the high oxidation state transition

* To whom correspondence should be addressed. E-mail: phillips@hkucc.hku.hk; ceszhcy@mail.sysu.edu.cn.

[†] The University of Hong Kong.

[‡] Sun Yat-Sen University.

(1) (a) Janowicz, A. H.; Bergman, R. G. *J. Am. Chem. Soc.* **1982**, 104, 352. (b) Arndtsen, B. A.; Bergman, R. G.; Monley, T. A.; Peterson, T. H. *Acc. Chem. Res.* **1995**, 28, 154.

(2) Shilov, A. E.; Shul'pin, G. B. *Chem. Rev.* **1997**, *97*, 2879.

(3) Labinger, J. A.; Bercaw, J. E. *Nature* **2002**, *417*, 507.

(4) Davies, H. M. L.; Beckwith, R. E. J. *Chem. Rev.* **2003**, *103*, 2861.

(5) (a) Armentrout, P. B.; Baer, T. *J. Phys. Chem.* **1996**, *100*, 12866. (b) Freiser, B. S., Ed. *Organometallic Ion Chemistry*; Kluwer Academic Publishers: Dordrecht, 1996. (c) Capron, L.; Mestdagh, H.; Rolando, C. *Coord. Chem. Rev.* **1998**, *178–180*, 269. (d) Armentrout, P. B. In *Topics in Organometallic Chemistry*; Brown, J. M., Hofmann, P., Eds.; Springer-Verlag: Berlin, 1999; Vol. 4, pp 1–45. (e) Schwarz, H. *Pure Appl. Chem.* **2000**, *72*, 2319. (f) Fisher, K. J. *Prog. Inorg. Chem.* **2001**, *50*, 343. (g) Armentrout, P. B. *Annu. Rev. Phys. Chem.* **2001**, *52*, 423.

(6) (a) Irikura, K. K.; Beauchamp, J. L. *J. Am. Chem. Soc.* **1991**, *113*, 2769.

(7) Schwarz, H. *Angew. Chem., Int. Ed. Engl.* **1991**, *30*, 820.

(8) (a) Hendrickx, M.; Ceulemans, M.; Gong, K.; Vanquickenborne, L. *J. Phys. Chem. A* **1997**, *101*, 2465. (b) Yoshizawa, K.; Suzuki, A.; Yamabe, T *J. Am. Chem. Soc.* **1999**, *121*, 5266. (c) Yoshizawa, K. *J. Organomet. Chem.* **2001**, *635*, 100.

(9) Bloomberg, M. R. A.; Siegbahn, P. E. M.; Svensson, M. *J. Phys. Chem.* **1994**, *98*, 2062.

(10) (a) Irikura, K. K.; Goddard, W. A. *J. Am. Chem. Soc.* **1994**, *116*, 8733. (b) Heinemann, C.; Hertwig, R. H.; Wesendrup, R.; Koch, W.; Schwarz, H. *J. Am. Chem. Soc.* **1995**, *117*, 495.

(11) (a) Crabtree, R. H. *Chem. Rev.* **1985**, *85*, 245–269. (b) Crabtree, R. H. *Chem. Rev.* **1995**, *95*, 9870.

10.1021/om7007452 CCC: $40.75
Publication on Web 12/27/2007

metal complexes containing a carbon-metal double or triple bond for the development of catalysts to accomplish alkane activation reactions and to perform catalytic metathesis of alkenes, alkynes, and cyclic compounds.[12–18] However, the activation of alkanes (such as CH_4) by naked neutral transition metals and their ions involve several electronic states that may also have different spins, and this complicates unraveling the C-H bond activation process. This phenomenon of "multiple-state reactivity" has been recognized for inorganic, organometallic, and bioinorganic reactions,[19–21] and much of the discussion of these systems has remained qualitative because standard computational methods did not allow for the easy location of critical points for these processes. Therefore, the minimum energy crossing points (MECPs) between states of different spin have been hard to characterize until recently. Increased computational resources and new algorithms now enable MECPs to be located for large, realistic systems containing transition metals, and now computational studies are able to help provide important new insight into the mechanism of reactions like the oxidation of C-H bonds to metal centers.

Previous studies on the reactions between transition metal atoms and methane have shown that inversion of the C-H bond of methane is more facile for metal cations than for neutral metal atoms. Thus, numerous transition metal ions have been employed to investigate the activation of small alkanes in the gas phase. For example, the first- and the second-row M^+ (M = Fe, Mn, and Zr) and the third-row M^+ (M = Ta, W, Os, Ir, and Pt)[22,23] have all been studied experimentally and/or theoretically. In contrast, there have been relatively few reports involving the reaction of neutral transition metal M atoms with small alkanes until recently. This can largely be attributed to the strong C-H bond in the methane compared to many other hydrocarbons (e.g., the C-H bond energy in methane is about 105 kcal mol^{-1}). Fortunately, recent experiments by Andrews and co-workers using the laser-ablation matrix infrared method have shown that the early transition metals in groups IV and VI react with methyl halides and methane to produce the simplest methylidene (CH_2=MHX, X = H, F, Cl, and Br) and methylidyne (CH≡MH_2X) complexes along with the metal methyl hydride or halide (CH_3-MX) complexes.[24–35] This work provides a simple model system to study substituent effects on the C-H activation of methane and its derivatives. In 1992 Blomberg and co-workers theoretically investigated the mechanisms for reactions between methane and the neutral transition metal atoms from yttrium to palladium. This study helped to explain why the barrier for the C-H insertion reaction is the lowest in energy for rhodium atoms (only for the initial C-H insertion step of the reaction).[36–39] To our knowledge, a detailed potential energy surface for the activation of methane by neutral molybdenum atoms has not been reported. In this article, we report a density functional theory (DFT) study of the reactions of methane with neutral molybdenum atoms. The potential energy surfaces and crossing seams associated with the C-H activation of methane by Mo atoms were examined, and important new insight into the mechanism of the reactions was achieved. We found that C-H activation of methane by Mo atoms involves "two- or multiple-state reactivity" based on our DFT calculations and the lowest energy pathway was determined to be ^{5}Mo + CH_4 → CH_3—MoH (^{5}**1**) → CH_2=MoH_2 (^{3}**2**) → CH≡MoH_3 (^{1}**3**). To better understand the spin inversion processes involved in the C-H bond activation reaction, we determined the energies and structures of the crossing points between the two potential energy surfaces (PESs) of different spin states in the reaction pathway. The effect of the crossing points on the energy barriers of the different reaction pathway steps is discussed, and we compare our computational results to the experimental results reported previously by Andrews and co-workers for the C-H bond activation of methane by Mo atoms.[31]

2. Computational Details

We optimized local minima on the potential energy hypersurfaces corresponding to the reactant complex, the reaction intermediates, the final complex, and other fragment species by employing the B3LYP density functional theory method.[40] The spin-unrestricted version of this methodology was used for all of the calculations. Vibrational analyses were systematically carried out in order to ensure that all of the optimized geometries correspond to a local minimum that has no imaginary frequency mode or to a saddle point that has only one imaginary frequency mode. In all of the calculations, the 6-311++G (3df, 3pd) basis set was used for the carbon and hydrogen atoms, and the sdd basis set was used for the Mo atoms.[41] Intrinsic reaction coordinates (IRCs) were traced from a

(12) Legzdins, P.; Tran, E. *J. Am. Chem. Soc.* **1997**, *119*, 5071.
(13) Buchmeiser, M. R. *Chem. Rev.* **2000**, *100*, 1565.
(14) Crabtree, R. H. *Chem. Rev.* **1985**, *85*, 245.
(15) Crabtree, R. H.; Hamilton, D. G. *Adv. Organomet. Chem.,* **1988**, *28*, 299.
(16) Zhang, K.; Gonzalez, A. A.; Mukerjee, S. L.; Chou, S. J.; Hoff, C. D.; Kubat-Martin, K. A.; Barnhart, D.; Kubas, G. J. *J. Am. Chem. Soc.* **1991**, *113*, 9170.
(17) Ujaque, G.; Cooper, A. C.; Maseras, F.; Eisenstein, O.; Caulton, K. G. *J. Am. Chem. Soc.* **1998**, *120*, 361.
(18) Wada, K.; Craig, B.; Pamplin, C. B.; Legzdins, P.; Patrick, B. O.; Tsyba, I.; Bau, R. *J. Am. Chem. Soc.* **2003**, *125*, 7035.
(19) Gutlich, P.; Garcia, Y.; Woike, T. *Coord. Chem. Rev.* **2001**, *219*, 839.
(20) Gutlich, P.; Garcia, Y.; Goodwin, H. A. *Chem. Soc. Rev.* **2000**, *29*, 419.
(21) Harvey, J. N.; Poli, R.; Smith, K. M. *Coord. Chem. Rev.* **2003**, *238*, 347.
(22) (a) Buckner, S. W.; McMahon, T. J.; Byrd, G. D.; Freiser, B. S. *Inorg. Chem.* **1989**, *28*, 3511. (b) Ranasinghe, Y. A.; MacMahon, T. J.; Freiser, B. S. *J. Phys. Chem.* **1991**, *95*, 7721.
(23) Irikura, K. K.; Beauchamp, J. L. *J. Am. Chem. Soc.* **1989**, *111*, 75.
(24) Cho, H.-G.; Andrews, L. *J. Phys. Chem. A* **2004**, *108*, 6294 (Ti + CH_3F).
(25) Cho, H.-G.; Andrews, L. *J. Am. Chem. Soc.* **2004**, *126*, 10485 (Zr + CH_3F).
(26) Cho, H.-G.; Andrews, L. *Organometallics* **2004**, *23*, 4357 (Hf + CH_3F).
(27) Cho, H.-G.; Andrews, L. *Inorg. Chem.* **2005**, *44*, 979 (Ti + CH_3X).
(28) Andrews, L.; Cho, H.-G.; Wang, X. *Angew. Chem., Int. Ed* **2005**, *44*, 113 (Zr + CH_4).
(29) Cho, H.-G.; Wang, X.; Andrews, L. *J. Am. Chem. Soc.* **2005**, *127*, 465 (Zr + CH_4).
(30) Cho, H.-G.; Wang, X.; Andrews, L. *Organometallics* **2005**, *24*, 2854 (Hf + CH_4).
(31) Cho, H.-G.; Andrews, L. J. *Am. Chem. Soc* **2005**, *127*, 8226 (Mo + CH_4).
(32) Andrews, L.; Cho, H.-G.; Wang, X *Inorg. Chem.* **2005**, *44*, 4834 (Ti + CH_4).
(33) Cho, H.-G.; Andrews, L. *Chem. Eur. J.* **2005**, *11*, 5017 (Mo + CH_3F).
(34) Cho, H.-G.; Andrews, L. *Organometallics* **2005**, *24*, 5678 (W + CH_3F).
(35) Cho, H.-G.; Andrews, L. *Organometallics* **2006**, *25*, 477.
(36) Blomberg, M. R. A.; Siegbahn, P. E. M. *Organometallics* **1994**, *13*, 354.
(37) Auffer, H. U.; Hinrichs, R. Z.; Schroden, J. J. *J. Phys. Chem. A* **2000**, *104*, 1107.
(38) Blomberg, M. R. A.; Siegbahn, P. E. M.; Svensson, M. *J. Am. Chem. Soc.* **1992**, *114*, 6095.
(39) Theodoor de Jong, G. *J. Chem. Phys.* **2004**, *121*, 9982.
(40) (a) Becke, A. D. *J. Chem. Phys.* **1993**, *98*, 5648. (b) Becke, A. D. *Phys. Rev. A* **1988**, *38*, 3098. (c) Vosko, S. H.; Wilk, L.; Nusair, M. *Can. J. Phys.* **1980**, *58*, 1200. (d) Lee, C.; Yang, W.; Parr, R. G. *Phys. Rev. B* **1988**, *37*, 785.
(41) (a) McLean, A. D.; Chandler, G. S. *J. Chem. Phys.* **1980**, *72*, 5639. (b) Krishnan, R.; Binkley, J. S.; Seeger, R.; Pople, J. A. *J. Chem. Phys.* **1980**, *72*, 650.

transition state toward both the reactant and product directions using an algorithm developed by Gonzalez and Schlegel in the mass-weighted internal coordinate system.[42] Each IRC is constructed from an accuracy of 0.1 $amu^{1/2}\cdot bohr$. All of the calculations were performed using the Gaussian 98 Program.[43]

3. Results and Discussions

The activation of methane by laser-ablated molybdenum atoms to form CH_3—MoH (^{5}**1**), CH_2═MoH_2(^{3}**2**), and CH≡MoH_3 (^{1}**3**) complexes appears to have three H-transfers on the reaction pathways. H_1, H_2, and H_3 are used in the rest of the paper to denote these three hydrogen atoms in order to keep the discussion more simple, and each species is labeled with its spin multiplicity as a superscript preceding the formula without its spatial symmetry. Initially, the Mo atom reaction with methane apparently takes place with excited ^{5}Mo atoms formed in the laser ablation process or by the direct laser irradiation employed during the laser ablation. The possible starting material (we note that on the basis of the laser-ablation matrix infrared method, the reaction could also possibly initiate from an activated species such as triplet Mo + CH_4 and singlet Mo + CH_4 in the reaction system, and the activation process may also possibly involve a spin inversion during the first C-H activation step), excited ^{5}**0** (^{5}Mo + CH_4), is calculated to be lower in energy than the excited triplet reactant complex ^{3}**0** (^{3}Mo + CH_4) and the singlet reactant complex ^{1}**0** (^{1}Mo–CH_4) by 20.3 and 52.8 kcal mol^{-1}, respectively. The ^{5}Mo atom reaction with methane to form the CH_3—MoH (^{5}**1**) intermediate via the first H_1-transfer requires some activation energy to start the C-H activation process. Subsequently, the excited intermediate can then be relaxed by the surrounding molecules in the matrix to form the ground state CH_3—MoH (^{5}**1**) intermediate or perhaps undergo the second H_2-transfer to form the methylidene complex CH_2═MoH_2 (^{5}**2**) and then proceed further to CH_2═MoH_2(^{3}**2**). Finally, the third H_3-transfer seems to take place from the excited CH_2═MoH_2 (^{3}**2**) complex to produce the CH≡MoH_3 (^{3}**3**) intermediate that then subsequently forms CH≡MoH_3 (^{1}**3**).

The potential energy profiles for the quintet, triplet, and singlet states were determined to investigate the possible spin crossovers involved in the reaction pathways. The calculated potential energy profiles for the quintet, triplet, and singlet states and the optimized geometries for all of the stationary points on the three potential energy profiles are shown in Figure 1. The free energy, the relative energy, and the relative energy including the zero-point vibrational energy (ZPVE) for the reaction pathways are collected in Table 1.

A. Overview of the Potential Energy Surfaces for the Three Possible States. The calculated potential energy profiles are shown in Figure 1, part a for the quintet, part b for the triplet, and part c for the singlet. As for the quintet surface, the reactants (methane and the excited quintet Mo atom (^{5}Mo + CH_4)), ^{5}**0**, proceeds to form the hydridomethyl complex CH_3—MoH (^{5}**1**) through the transition state ^{5}**TS$_{0-1}$**. The first H_1-transfer is exothermic by 25.4 kcal mol^{-1} and has a barrier of 10.3 kcal mol^{-1}. The next step is the second H_2-transfer of ^{5}**1** to generate the methylidene dihydride complex CH_2═MoH_2 (^{5}**2**) via the transition state ^{5}**TS$_{1-2}$**. This step has a reaction barrier of 51.0 kcal mol^{-1}. Finally, the H_3-transfer leads to the possible CH≡MoH_3 (^{5}**3**) methylidyne complex from the complex CH_2═MoH_2 (^{5}**2**), via the transition state ^{5}**TS$_{2-3}$**. This step is endoergic by 47.0 kcal mol^{-1} and has a barrier of 51.0 kcal mol^{-1}. To summarize, the second H_2-transfer and the third H_3-transfer, with barriers of 51.0 kcal mol^{-1}, are the rate-determining steps on the pure quintet reaction pathway. The overall reaction on this pathway is endoergic by 61.0 kcal mol^{-1} and is not very easy to take place for the H_2- and H_3-transfer steps.

With respect to the triplet state pathway, the first step of the reaction on the triplet PES starts with the reactants (triplet Mo and methane (^{3}Mo + CH_4)), ^{3}**0**, which is 20.3 kcal mol^{-1} in energy above the reactants ^{5}**0**. The second step is the formation of the hydridomethyl complex CH_3—MoH (^{3}**1**), via the transition state ^{3}**TS$_{0-1}$**. This H_1-transfer step is exothermic by 16.0 kcal mol^{-1} and has a barrier of 7.1kcal mol^{-1}. Next, the complex CH_3—MoH (^{3}**1**) proceeds with the second H_2-transfer to produce the triplet methylidene complex CH_2═MoH_2 (^{3}**2**), which is exothermic by 14.1 kcal mol^{-1} and has an activation barrier of only 4.2 kcal mol^{-1}. Finally, the activation of the third C-H_3 bond via the transition state ^{3}TS_{2-3} produces the methylidyne complex CH≡MoH_3 (^{3}**3**). This step is endoergic by 37.2 kcal mol^{-1} and has a barrier of 40.8 kcal mol^{-1}. Analysis of the triplet potential energy profile shows that the methylidene complex CH_2═MoH_2 is easy to be formed with a low barrier of 4.2 kcal mol^{-1}. However, the formation of the methylidyne complex CH≡MoH_3 on the triplet PES is difficult due to its high reaction barrier of 40.8 kcal mol^{-1}.

The singlet state pathway is shown in Figure 1c. As compared with that of ^{5}**0**, the complex formed (^{1}Mo–CH_4), ^{1}**0**, from methane and the excited state ^{1}Mo is higher in relative energy by 52.8 kcal mol^{-1}. Then the hydridomethyl complex ^{1}**1** is formed via a H_1-transfer through the transition state ^{1}**TS$_{0-1}$**, with a reaction barrier of 0.6 kcal mol^{-1}. Subsequently, the H_2 and H_3 transfer reactions take place on the corresponding complexes via transition states ^{1}**TS$_{1-2}$** and ^{1}**TS$_{2-3}$**, respectively. The oxidative addition of the second C-H_2 bond and the third C-H_3 bond to form the methylidene complex ^{1}**2** and the methylidyne complex ^{1}**3** are facile on the singlet pathway with barriers to reaction of 4.0 and 0.4 kcal mol^{-1}, respectively. These low barriers are noticeably different from those for the corresponding reactions that occur on the quintet and triplet state pathways. The rate-determining step on the singlet state PES is the H_2 transfer from methane to ^{1}Mo.

As shown in Figure 2, we find that the excited state of reactants ^{5}Mo + CH_4 (^{5}**0**) generates the most stable hydridomethyl complex CH_3—MoH (^{5}**1**). The ground state of intermediate **1** is located as ^{5}A′, which is in good agreement with the results of Boomberg and co-workers,[38] as well as the results of Andrew and co-workers calculated with B3LYP density functional theory, 6-311++G(3df,3pd).[31] However, among the methylene complexes, the triplet species ^{3}**2** has the lowest energy. For the methylidyne species examined, the relative order of stability is observed to be ^{1}**3** > ^{3}**3** > ^{5}**3**. Therefore, if methane is readily activated by the excited state ^{5}Mo, as observed experimentally,

(42) (a) Gonzalez, C.; Schlegel, H. B. *J. Phys. Chem.* **1990**, *94*, 2154. (b) Gonzalez, C.; Schlegel, H. B. *J. Phys. Chem.* **1990**, *94*, 5523.

(43) Frisch, M. J.; Trucks, G. W.; Schlegel, H. B.; Scuseria, G. E.; Robb, M. A.; Cheeseman, J. R.; Zakrzewski, V. G.; Montgomery, J. A., Jr., Stratmann, R. E.; Burant, J. C.; Dapprich, S.; Millam, J. M.; Daniels, A. D.; Kudin, K. N.; Strain, M. C.; Farkas, O.; Tomasi, J.; Barone, V.; Cossi, M.; Cammi, R.; Mennucci, B.; Pomelli, C.; Adamo, C.; Clifford, S.; Ochterski, J.; Petersson, G. A.; Ayala, P. Y.; Cui, Q.; Morokuma, K.; Malick, D. K.; Rabuck, A. D.; Raghavachari, K.; Foresman, J. B.; Cioslowski, J.; Ortiz, J. V.; Baboul, A. G.; Stefanov, B. B.; Liu, G.; Liashenko, A.; Piskorz, P.; Komaromi, I.; Gomperts, R.; Martin, R. L.; Fox, D. J.; Keith, T.; Al-Laham, M. A.; Peng, C. Y.; Nanayakkara, A.; Gonzalez, C.; Challacombe, M.; Gill, P. M. W.; Johnson, B.; Chen, W.; Wong, M. W.; Andres, J. L.; Gonzalez, C.; Head-Gordon, M.; Replogle, E. S.; Pople, J. A. *Gaussian 98, revision A.7* and *Gaussian 03, revision B.05*; Gaussian Inc.: Pittsburgh, PA, 1998, 2003.

(44) Singleton, D. A.; Szymanski, M. J.; Hall, M. B. *J. Am. Chem. Soc.* **2001**, *123*, 9822.

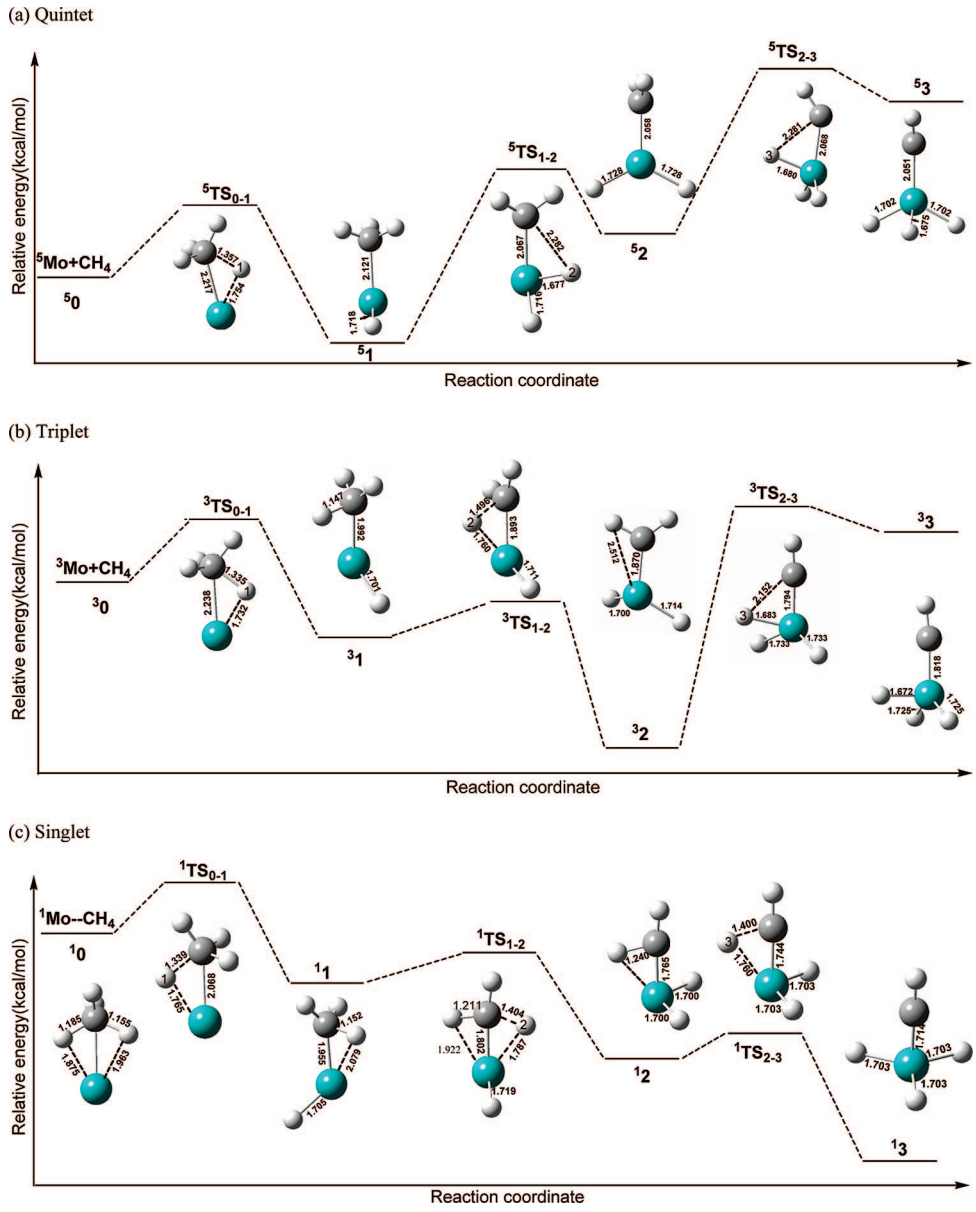

Figure 1. B3LYP potential energy surfaces and selected bond lengths in angstroms for the stationary points of the reaction Mo + CH_4 on the quintet (a), triplet (b), and singlet (c) state surfaces, respectively.

Table 1. B3LYP/6-311++G (3df,3pd) :sdd Calculated ΔE_{elec}, ΔE_{rel}, and ΔG_{298} for Stationary Structures Located on the Quintet, Triplet, and Singlet State PESs[a]

	Quintet			Triplet			Singlet		
species	ΔE_{elec}	ΔE_{rel}	ΔG_{298}	ΔE_{elec}	ΔE_{rel}	ΔG_{298}	ΔE_{elec}	ΔE_{rel}	ΔG_{298}
0 (CH_4 ± Mo)	0[b]	0[c]	0[d]	20.28	20.28	20.59	52.76	51.07[e]	57.69[e]
TS_{0-1}	10.32	6.90	12.32	27.39	23.96	29.45	53.37	49.51	56.33
1	−25.35	−28.76	−23.36	4.27	0.34	6.26	20.85	16.45	22.86
TS_{1-2}	25.66	18.52	24.20	8.44	1.86	7.95	24.85	17.46	24.31
2	14.07	7.38	12.87	−9.81	−16.26	−10.43	6.93	0.54[e]	7.43[e]
TS_{2-3}	65.06	54.74	60.17	30.98	21.68	27.77	7.34	−0.11	6.85
3	61.03	51.64	57.04	27.47	18.82	24.66	−10.74	−17.14	−10.23

[a] ΔE_{elec} = relative energy (kcal mol^{-1}), ΔE_{rel} = relative energy with correction of the zero-point energy (kcal mol^{-1}), and ΔG_{298} = free energy in the gas phase (kcal mol^{-1}). [b] Absolute energy E = −108.60272 au. [c] Absolute energy E = −108.558159 au. [d] Absolute energy E = −108.594779 au. [e] A value that reflects the error in the harmonic approximation for the calculating the zero-point energy.[44]

there must be some surface crossings between the quintet and triplet surfaces as well as the triplet and singlet reaction surfaces, caused by the spin-orbital coupling to provide an overall reaction pathway consistent with experimental observations.

B. Geometries and Stabilities of Stationary Points. The lowest quintet state of Mo has a $4d^55s^1$ electron configuration with one 4d orbital that is doubly occupied. The lowest triplet state of Mo has two 4d orbitals that are doubly occupied and also has a $4d^55s^1$ electron configuration. The lowest singlet state of Mo has three 4d orbitals that are doubly occupied, and its electron configuration is $4d^65s^0$. The difference between these states of Mo can be used to quantitatively understand the

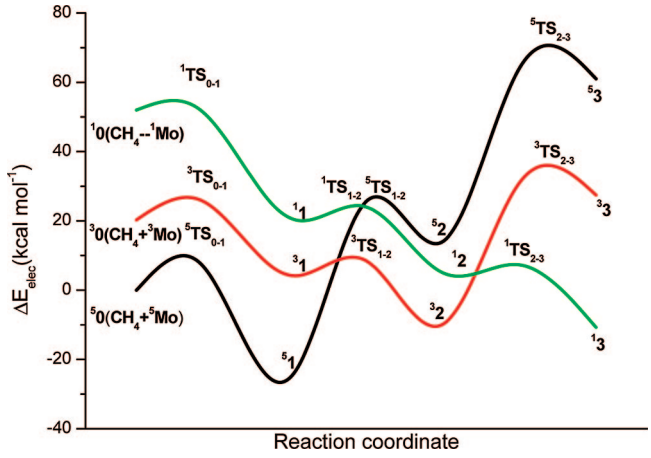

Figure 2. B3LYP potential energy surfaces of the reaction ^{5}Mo + $CH_4 \rightarrow CH_3$—MoH (^{5}**1**) $\rightarrow CH_2$=MoH_2 (^{3}**2**) $\rightarrow$ CH≡MoH_3(^{1}**3**) on the quintet, triplet, and singlet state surfaces.

insertion reactivity of Mo into the C-H bond of methane. As is well-known, the oxidative addition of a C-H bond to a Mo center is proceeded by donation of the bonding σ electrons of the C-H bond into the vacant 5s or $4d_\sigma$ orbitals of Mo and back-donation of the Mo $4d_\pi$ electrons into the antibonding σ^* orbital of the C-H bond. The 5s electrons are the most diffuse electrons in the metal, and therefore the lower the number of 5s electrons in the configuration, the smaller the repulsion. This is consistent with our present results for the reaction of Mo with methane. For the lowest quintet state Mo and the triplet state Mo that have the least empty 5s and $4d_\sigma$ orbitals, there is no corresponding η^2-complexes between Mo and methane found in the above two states. In contrast to the behavior of the quintet and triplet reaction between Mo and methane, molecular orbital considerations predict that the excited state ^{1}Mo approach to methane forms a tight or strongly bound complex. Interestingly, our calculated result also has a good agreement with the molecular orbital prediction. For example, the complex (^{1}**0**) obtained from the DFT calculation at the theory of B3LYP is shown in Figure 1. The distances between Mo and the two hydrogen atoms are 1.875 and 1.963 Å, respectively. Because of the η^2-complexes between Mo and methane, the corresponding C-H bonds show agostic character. The C-H bond lengths are calculated to be 1.185 and 1.155 Å, respectively, which are significantly longer than the normal C-H bond length in methane.

Along the quintet, triplet, and singlet state pathways of the oxidative addition of the C-H_1 bond to the Mo metal, we have located three transition states, namely, ^{5}**TS$_{0-1}$**, ^{3}**TS$_{0-1}$** and ^{1}**TS$_{0-1}$**, respectively. ^{5}**TS$_{0-1}$** on the quintet state pathway and ^{3}**TS$_{0-1}$** on the triplet state pathway are three-centered transition states. ^{5}**TS$_{0-1}$** is 17.1 kcal mol^{-1} lower in energy than ^{3}**TS$_{0-1}$**. However, the ^{1}**TS$_{0-1}$** on the singlet state pathway has a four-centered coordination mode. ^{1}**TS$_{0-1}$** is 26.0 and 43.1 kcal mol^{-1} higher in energy than ^{3}**TS$_{0-1}$** and ^{5}**TS$_{0-1}$**, respectively.

Examination of the stabilities of the spin state species of the hydridomethyl intermediate **1** shows that the ground state of intermediate **1** is a quintet state (i.e., ^{5}**1**) that is 29.6 and 46.2 kcal mol^{-1} lower in relative energy than those for ^{3}**1** and ^{1}**1**, respectively. The ^{5}A′ ground state determined for the hydridomethyl intermediate **1** has a similar structure to the located ^{3}A′; structure for the triplet hydridomethyl intermediate ^{3}**1**. The energy difference between them is calculated to be 20.2 kcal mol^{-1}, and this is in excellent agreement with the computational results of Andrews and co-workers (20 kcal mol^{-1}).[31] NBO calculations show that the energy differences associated with ^{5}**1**, ^{3}**1**, and ^{1}**1** can be mostly understood in terms of the electronic configurations associated with the metal in these three species. Among them, one 5s and one 4d orbital are involved in the formation of the two covalent bonds. The other four 4d orbitals are all singly occupied in ^{5}**1**, and all of them have the same spin. However, one and two of the unpaired electrons must flip over in ^{3}**1** and ^{1}**1** to ensure the triplet and singlet multiplicity of these species, respectively. Thus, the observed destabilization of the ^{3}**1** and ^{1}**1** complexes relative to the ^{5}**1** complex is likely mainly caused by the loss of some quantum mechanical exchange effects. Evidence can also be seen from the structures of the different spin state species of the hydridomethyl intermediate **1**. Since there are no vacant 4d orbitals on the Mo center of ^{5}**1**, the formed quintet hydridomethyl intermediate ^{5}**1** has no C-H agostic interaction. However, in the triplet and singlet hydridomethyl intermediates ^{3}**1** and ^{1}**1**, the vacant 4d orbital can interact with the C-H bond of the methyl moiety. For example, one of the C-H bonds of the methyl has been elongated to become 1.147 Å in ^{3}**1** and 1.152 Å in ^{1}**1**, respectively.

We have located three spin state species for the methylene dihydride species **2**, namely, the quintet ^{5}**2**, triplet ^{3}**2**, and singlet ^{1}**2**. The triplet ^{3}**2**, is the ground state (^{3}A) for the methylene dihydride species **2**, which is calculated to be higher in energy by 15.5 kcal mol^{-1} than the ground state hydridomethyl intermediate (^{5}**1**). This is in good agreement with the computational energy difference of these two species by Cho and Andrews.[31] The calculated ^{5}**2** and ^{1}**2** species are 23.9 and 16.7 kcal mol^{-1} higher in energy, respectively, than the ^{3}**2** species. The stabilities of the methylene dihydride species **2** with different spin states can also be rationalized by the optimized geometries found for these species. Inspection of Figure 1 reveals that the Mo-C and Mo-H_2 bond distances are 2.06 and 1.73 Å in ^{5}**2**. However, the Mo=C and Mo-H_2 bond distances are 1.87 and 1.70 Å in ^{3}**2**, respectively. These structural parameters show that the Mo=C and Mo-H_2 bonds are quite strong in ^{3}**2** but relatively weak in ^{5}**2**. This leads to the ^{5}**2** species being 23.9 kcal mol^{-1} higher in energy than the ^{3}**2** species. The energy difference between the ^{3}**2** and ^{1}**2** species can also be attributed to their different electronic configurations determined from the NBO calculations. In both species, one 5s and three 4d orbitals are involved in the formation of four covalent bonds, while the other two 4d orbitals in ^{3}**2** are all singly occupied and one of them has to flip over in ^{1}**2** to ensure a singlet multiplicity for the ^{1}**2** species. The destabilization of the ^{1}**2** over ^{3}**2** species is also likely mainly due to the loss of quantum mechanical exchange effects. In the methylene dihydride species ^{5}**2** and ^{3}**2**, there is no vacant 4d orbital on the Mo center. In contrast, the vacant 4d orbital on the Mo center of ^{1}**2** can attract the σ bond electrons of the C-H bond of the methylene to form a C-H agostic bond. As shown in Figure 1c, one of the C-H bonds of the methylene has been enlongated to 1.240 Å in ^{1}**2**. This kind of agostic interaction may contribute significantly to the third H_3-transfer step.

The second H_2-transfer step of hydridomethyl complex CH_3—MoH (**1**) to generate the methylidene dihydride complex CH_2=MoH_2 (**2**) needs to go though the transition state **TS$_{1-2}$**. We have located three transition states, namely, ^{5}**TS$_{1-2}$**, ^{3}**TS$_{1-2}$**, and ^{1}**TS$_{1-2}$** on the quintet state, triplet state, and singlet state pathways. Interestingly, the ^{5}**TS$_{1-2}$** and ^{3}**TS$_{1-2}$** are three-centered transition states, whereas ^{1}**TS$_{1-2}$** is a four-centered transition state caused by its singlet spin multiplicity. Analysis of these structural parameters shows that ^{3}**TS$_{1-2}$** and ^{1}**TS$_{1-2}$** are relatively

early transition states (e.g., the C−H_2 bond lengths are 1.50 and 1.40 Å, respectively) and thus have small barriers of 4.2 and 4.0 kcal mol^{-1} on the triplet state and singlet state pathways, respectively. ^{5}**TS$_{1-2}$** is a very late transition state (the C−H_2 bond length is 2.28 Å) with a high barrier to reaction of 51.0 kcal mol^{-1} on the quintet state pathway. The relative order of the stability of the methylene complex species is ^{3}**2** > ^{1}**2** > ^{5}**2**. The relatively small barrier on the triplet state pathway can be rationalized by the fact that the triplet state is not optimal for the hydridomethyl complex but appears optimal for the methylene dihydride complex.

The geometries of the methylidyne species show that the C≡Mo in ^{1}**3** is 1.71 Å. The bond lengths are shorter than those in ^{5}**3** (2.05 Å) and in ^{3}**3** (1.82 Å). The relative order of the strengths of the formed Mo-C clearly indicated that the relative order of stability of the methylidyne complex CH≡MoH_3 (**3**) is ^{1}**3** > ^{3}**3** > ^{5}**3**. The calculations show that ^{1}**3** is 71.8 and 38.2 kcal mol^{-1} lower in the relative energy than ^{5}**3** and ^{3}**3**, respectively. Additionally, this calculated ground state methylidyne species ^{1}**3** is 11.6 kcal mol^{-1} higher in relative energy with ZPE correction than ^{5}**1** and 0.9 kcal mol^{-1} lower in relative energy with ZPE correction than ^{3}**2**. These results are quite consistent with the computational results by Cho and Andrews.[31] Again, it is instructive to give a concise and qualitative description of the bonding mode in these species. In ^{1}**3** the Mo atom uses one 5s orbital and five 4d orbitals to form three normal covalent bonds with the hydrides and one triple bond with the carbon atom. The optimal bonding mode of the methylidyne complex Mo(VI) is obviously the one with the singlet spin multiplicity. In contrast to the bonding mode in ^{1}**3**, the triple-bond character of the Mo-C bond is reduced to some extent in ^{3}**3**, and the Mo-C bond has single bond character in ^{5}**3.** Thus, the weaker stability of ^{5}**3** and ^{3}**3** can probably be explained by the strength of the Mo-C bond in these compounds.

The third H_3-transfer step of methylidene dihydride complex CH_2=MoH_2 (**2**) to generate the methylidyne complex CH≡MoH_3 (**3**) needs to go though the transition state **TS$_{2-3}$**. We have located three transition states, namely, ^{5}**TS$_{2-3}$**, ^{3}**TS$_{2-3}$**, and ^{1}**TS$_{2-3}$** on the quintet state, triplet state, and singlet state pathways. The **TS$_{2-3}$** saddle point is the oxidative addition transition state for the C-H_3 bond to the Mo center. ^{5}**TS$_{2-3}$** and ^{3}**TS$_{2-3}$** are all three-centered transition states with different spin multiplicities. As shown in Figure 1c, there is an agostic C-H bond in ^{1}**2** (C-H bond, 1.240 Å). However, there are no agostic C-H bonds in ^{3}**2** and ^{5}**2**. Therefore, ^{1}**TS$_{2-3}$** is an earlier transition state than ^{5}**TS$_{2-3}$** and ^{3}**TS$_{2-3}$** as compared with their corresponding starting material, the methylidene dihydride complex CH_2=MoH_2 (**2**), and the ^{1}**TS$_{2-3}$** is 57.7 and 23.6 kcal mol^{-1} lower in energy than ^{5}**TS$_{2-3}$** and ^{3}**TS$_{2-3}$**. This is rationalized by the fact that the singlet pathway is optimal for the methylidyne complex **3**.

C. Spin Crossing Processes and the Minimum Energy Reaction Pathway. Figure 2 depicts the computed potential energy diagrams for the activation of methane by the laser-ablated Mo in the quintet, triplet, and singlet states. Examination of Figure 2 shows that the different C-H bond processes display completely different preferences for the reaction barriers on the three energy surfaces. For example, the quintet potential energy diagram lies below the triplet PES and the singlet PES. The quintet PES provides a low-cost reaction pathway for the first C-H_1 bond transfer. However, the triplet and singlet PESs provide a relatively easy reaction pathway for the C-H_2 transfer and C-H_3 transfer processes, respectively. In the preceding discussion, we can see that the minimum energy overall PES is not one of the three PESs of a certain spin state. Thus, the crossing of adiabatic surfaces of different spins is likely involved in the overall C-H bond activation by the Mo atom. We note that transition metal mediated reactions very often occur on more than one PES. This has attracted some experimental and theoretical attempts in reaction systems that include 3d, 4d, and some 5d transition metals.

On the basis of the analysis of Figure 2, several spin crossings can be found to be possible along the optimal reaction pathway of the activation of CH_4 by a molybdenum atom. First, the reaction may start with the formation of the hydridomethyl complex ^{5}**1** on the quintet PES. Then, the quintet surface could likely cross the triplet surface somewhere between **1** and **TS$_{1-2}$** since ^{5}**TS$_{1-2}$** is too high in energy and the formation of the complex **2** is exothermic on the triplet PES instead of endoergic on the quintet PES. After ^{3}**2** is formed, the reaction may jump to the singlet PES between **2** and **TS$_{2-3}$** since ^{3}**TS$_{2-3}$** is 23.6 kcal mol^{-1} above ^{1}**TS$_{2-3}$**. Also, the complex **3** on the singlet PES is thermodynamically more favored than the corresponding triplet state species. To conclude, the minimum energy pathway may proceed as Mo + CH_4(^{5}**0**) → CH_3—MoH(^{5}**1**) → ^{3}TS_{1-2} → CH_2=MoH_2 (^{3}**2**) → ^{1}TS_{2-3} → CH≡MoH_3 (^{1}**3**), and we shall explore this possibility in the next section.

D. IRC Analysis for the Reaction Pathway and Crossing Points between the PESs of Different Spin Multiplicities. Here, we explore the PESs for the crossing seams and the spin inversion processes for the C-H bond activation of methane by a neutral Mo atom. The transition of spin multiplicity may be expected to occur from the quintet state to the triplet state in the region prior to **TS$_{1-2}$**. Spin inversion is a nonadiabatic process and requires an inspection for a crossing seam on the different potential energy surfaces. The potential energy of the system that consists of 6 atoms (Mo + CH_4) has more than 10 internal degrees of freedom, and this makes it difficult to perform a detailed inspection for a crossing seam without some simplification. Therefore, we chose an approach suggested by Yoshizawa[45] and Shuhua Li[46] for approximately locating the crossing points of two PESs with different multiplicities. The main idea for this method is to perform a series of single-point computations of one spin state along the IRC of the other spin state and vice versa. Such an analysis will help locate energy-minimum and -maximum crossing points.

We first tried to locate the crossing points between the quintet and triplet (or singlet) surfaces in the region from complex **1** to the transition state **TS$_{1-2}$**.

The lines in Figure 3 represent the computed potential energy profiles of the triplet and quintet states along the quintet IRC (from transition state **TS$_{1-2}$** to complex **1**) in Figure 3a and along the triplet state IRC in Figure 3b (from transition state **TS$_{1-2}$** to complex **1**). The IRC is traced from ^{5}**TS$_{1-2}$** or ^{3}**TS$_{1-2}$** (IRC = 0) toward complex **1** (IRC < 0). In Figure 3a, one can see that a crossing point is located at IRC = −1.2 with an energy of 21.5 kcal mol^{-1} relative to that of ^{5}**1**. The bond distance of C-Mo is about 2.04 Å, and the distance of the forming Mo-H_2 bond is about 1.70 Å in **SI$_{5-3}$**. According to the methodology of Yoshizawa and Li and co-workers, this is the energy-maximum crossing point. In Figure 3b, another crossing point **SII$_{3-5}$** is found at IRC = −0.5 with an energy about 4.5 kcal mol^{-1} higher than ^{5}**1**. The bond distance of C-Mo is about 1.91 Å, and the Mo-H_2 distance is 1.83 Å. The quintet and the triplet

(45) (a) Yoshizawa, K.; Shiota, Y.; Yamabe, T. *J. Chem. Phys.* **1999**, *111*, 538. (b) Yoshizawa, K.; Kagawa, Y. *J. Phys. Chem. A* **2000**, *104*, 9347.

(46) Zhang, G.-B.; Li, S.-H. *Organometallics* **2003**, *22*, 3820.

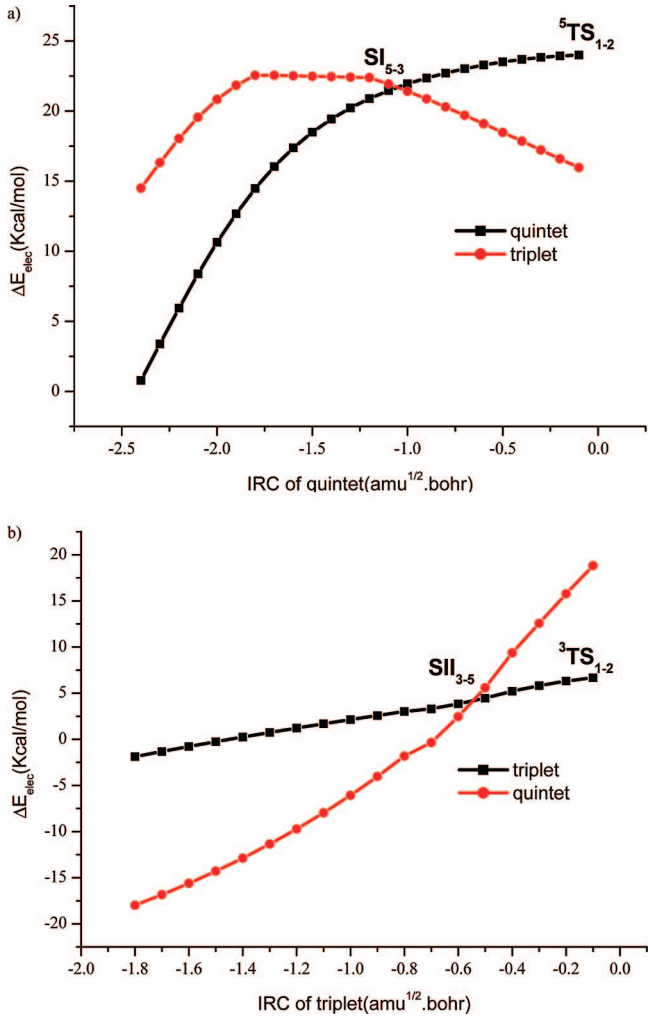

Figure 3. Potential energies along (a) the quintet from the methyl hydride (**1**) to the transition state ^{5}**TS$_{1-2}$** and (b) the triplet from the methyl hydride (**1**) to transition state ^{3}**TS$_{1-2}$**.

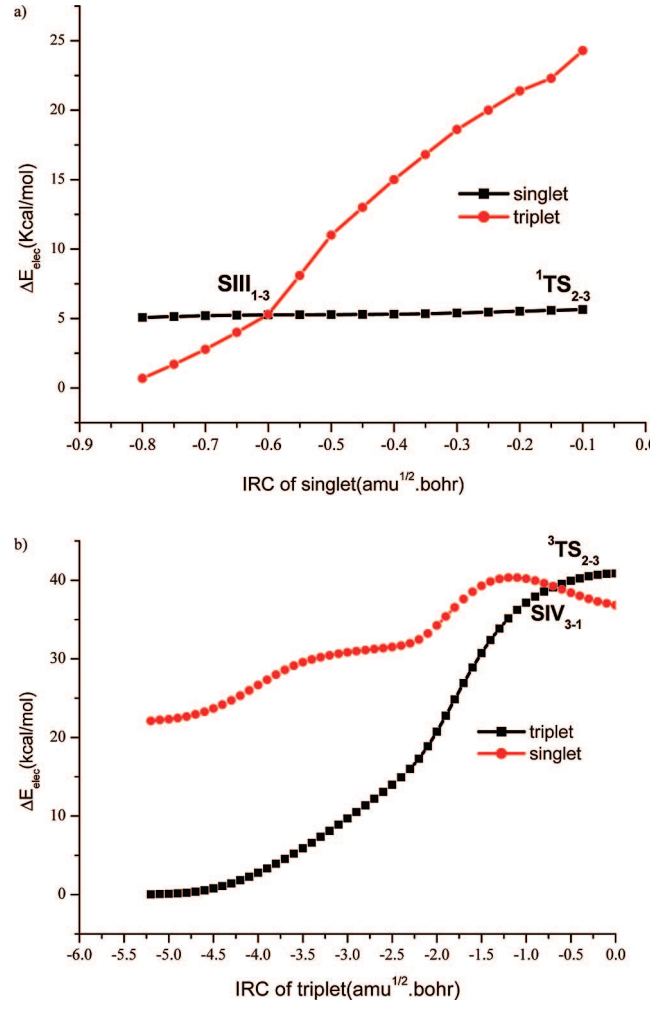

Figure 4. Potential energies from methylidene (**2**) to the transition state **TS$_{2-3}$** along (**3**): (a) the singlet and (b) the triplet states.

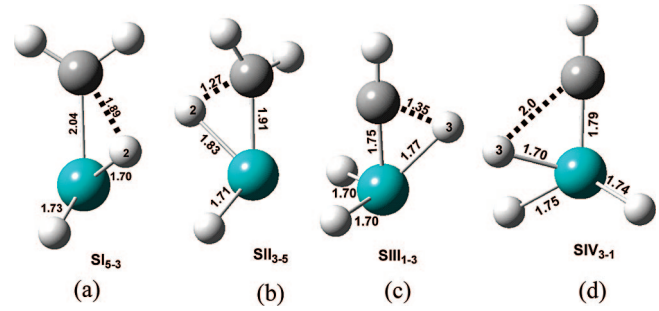

Figure 5. Structures of the crossing points: (a) the energy-maximum point between the quintet and triplet states before **TS$_{1-2}$**, (b) the energy-minimum point between the quintet and triplet states before **TS$_{1-2}$**, (c) the energy-minimum point between the singlet and triplet states before **TS$_{2-3}$**, and (d) the energy-maximum point between the singlet and triplet states before**TS$_{2-3}$**.

state potential energy surfaces can begin to touch at this point because the IRC valley of the quintet state still lies below that of the triplet state in this region of the reaction pathway. That is, **SII$_{3-5}$** is the energy-minimum crossing point between quintet and triplet surfaces in the reaction pathway from complex **1** to **TS$_{1-2}$**.The structures of both crossing points are given in Figure 5. Therefore, there is a crossing seam between **SI$_{5-3}$** and **SII$_{3-5}$**. The reacting system should change its spin multiplicities from the quintet state to the triplet state in this crossing region and then move on the triplet potential energy surface as the reaction proceeds. In summary, there is one crossing seam that is located between the quintet and the triplet state PESs, leading to a significant decrease in the barrier height of **TS$_{1-2}$** from 51.0 to 33.8 kcal mol^{-1} from complex **1** to complex **2** at the B3LYP level of theory.

Similarly, Figure 4 shows the potential energy surfaces of the triplet and singlet states from the methylene complex **2** to the transition state **TS$_{2-3}$** along the singlet and triplet IRCs, respectively. Two crossing points, **SIII$_{1-3}$** and **SIV$_{3-1}$**, between singlet and triplet PESs are located before **TS$_{2-3}$**. **SIII$_{1-3}$** is situated at IRC = −0.6 with a relative energy of 5.3 kcal mol^{-1} with respect to ^{3}**2**. At the point **SIII$_{1-3}$**, the complex is very similar to Cs structure, in which the bond distance of C-Mo is 1.75 Å and Mo-H$_3$ bond distance is 1.77 Å, this is an energy-minimum crossing point. **SIV$_{3-1}$** lies at IRC = −0.8 with a relative energy of 39.0 kcal mol^{-1} with respect to ^{3}**2**, which is an energy-maximum crossing point. The structures of both crossing points are also presented in Figure 5, and it has a C-Mo bond distance of 1.79 Å and a Mo-H bond distance of 1.70 Å. As seen in Figure 4, after passing the points **SIII$_{1-3}$** or **SIV$_{3-1}$**, the singlet PES can provide a low-energy reaction pathway toward the methylidyne complex **3**. Therefore, the reacting system is most likely to change its spin multiplicities from triplet to singlet state between these two crossing points without passing the transition state ^{3}**TS$_{2-3}$**. As a sequence, the barrier of activation of the third C-H$_3$ bond would decrease from 40.8

to 17.2 kcal mol^{-1}. In addition, analysis of the quintet and the singlet state potential energy profiles from complex **1** to $\mathbf{TS_{1-2}}$ shows that there is also a crossing seam from the energy-minimum point to the energy-maximum point. However, according to the approach of Yoshizawa,[31] one can see that before the crossing points of the quintet and the singlet potential energy profiles occur, the molecular system would preferentially move to the triplet PES from the quintet PES. Hence, this crossing seam would not likely play a significant role in the most probable reaction pathway from complex **1** to complex **2**, and therefore the corresponding energies and structures of this crossing point is not considered here.

4. Conclusion

IRC analysis of the C-H activation of methane by a laser-ablated Mo atom has been described. There are three main crossing seams on the quintet, triplet, and singlet states along the overall reaction pathway, and the reaction system would likely change its spin multiplicity twice in going from the entrance channel to the exit channel. The first spin inversion, from the quintet state to the triplet state, occurs between the crossing point $\mathbf{SI_{5-3}}$ and $\mathbf{SII_{3-5}}$, and after passing this point, the reaction system moves on the triplet PES toward the methylene complex **2**. An important consequence of this spin conversion is that the barrier of the second C-H_2 bond cleavage decreases from 51.0 to 33.8 kcal mol^{-1}. Analysis of Figure 2 shows that there is a crossing seam that exists between the methylene complex **1** and the transition state $\mathbf{TS_{1-2}}$ on the quintet and singlet PESs. This crossing point will not be important in the overall most probable reaction pathway because the triplet potential energy surface between complex **1** and transition state $\mathbf{TS_{1-2}}$ lies substantially below the quintet and singlet potential energy surface and accordingly the molecular system would preferentially move on the triplet potential energy surface before it could encounter this seam. The last likely spin conversion occurs from the triplet state to the singlet state near the crossing point $\mathbf{SIII_{1-3}}$ and $\mathbf{SIV_{3-1}}$. Subsequently, the reaction would prefer to proceed on the singlet potential energy surface until the completion of the reaction. This spin conversion leads to a decrease in the C-H_3 bond activation barrier height from 40.8 to 17.2 kcal mol^{-1}. The minimum energy reaction path is found not to be one of the three PESs associated with only one spin state. Instead, the minimum energy reaction path requires the crossing of two adiabatic surfaces with different spin states along the different reaction steps. We found that three spin states are involved in the overall most probable reaction pathway. The minimum energy pathway can be described as $^5Mo + CH_4$ (^{5}**0**) $\rightarrow$ $^5TS_{0-1} \rightarrow CH_3{-}MoH$ (^{5}**1**) $\rightarrow$ $^3TS_{1-2} \rightarrow CH_2{=}MoH_2$ (^{3}**2**) $\rightarrow$ $^1TS_{2-3} \rightarrow CH{\equiv}MoH_3$ (^{1}**3**).

Acknowledgment. This research has been supported by grants from the Research Grants Council of Hong Kong (HKU7021/03P), the award of a Croucher Foundation Senior Research Fellowship (2006–07) from the Croucher Foundation, and an Outstanding Researcher Award (2006) from the University of Hong Kong to D.L.P. and National Natural Science Foundation of China (Grant No. 20673149), the Scientific Research Foundation for the Returned Overseas Chinese Scholars, the State Education Ministry, and grants from the Sun Yat-Sen University to C.Y.Z.

Supporting Information Available: The optimized geometry for all of the reactants, reactant complexes, transition states, and product complexes obtained from the B3LYP/6-311++G(3df,3pd) calculations are shown for the reaction of $^5Mo + CH_4 \rightarrow$ $^5TS_{0-1} \rightarrow CH_3{-}MoH$ (^{5}**1**) $\rightarrow$ $^3TS_{1-2} \rightarrow CH_2{=}MoH_2$ (^{3}**2**) $\rightarrow$ $^1TS_{2-3} \rightarrow CH{\equiv}MoH_3$ (^{1}**3**). This material is available free of charge via the Internet at http://pubs.acs.org.

OM7007452